processes

MDPI

Article

Analyzing Energy Transfer Mechanism during Coal and Gas Protrusion in Deep Mines

Haitao Sun [1,2], Linchao Dai [1,2,*], Jun Lu [3,*], Jie Cao [1,2] and Minghui Li [3]

[1] State Key Laboratory of the Gas Disaster Detecting, Preventing and Emergency Controlling, Chongqing 400037, China
[2] China Coal Technology and Engineering Group, Chongqing Research Institute, Chongqing 400037, China
[3] Shenzhen Key Laboratory of Deep Underground Engineering Sciences and Green Energy, College of Civil and Transportation Engineering, Shenzhen University, Shenzhen 518060, China
* Correspondence: 20212001047g@cqu.edu.cn (L.D.); junlu@cqu.edu.cn (J.L.); Tel.: +86-02365239611 (L.D.)

Abstract: Coal is the mainstay of China's energy supply. With the gradual progress in China's policy of phasing out backward coal production capacity, the intensive and deep mining of coal has gradually become the new norm. The current mining depth is increasing at a rate of 10~15 m/year. The high crust stress, high gas pressure, high ground temperature, and engineering disturbance stress in deep coal mines can lead to the occurrence of coal–rock–gas dynamic disasters that are complex and show the characteristics of compound dynamic disasters. It is important to understand the evolution and mechanism of deep coal and rock dynamic disasters accurately for the safe development of deep resources. To study the mechanism of occurrence and the evolution of impact–protrusion compound dynamic disasters, we herein analyzed the apparent characteristics of coal–rock–gas compound dynamic disasters in deep mines and obtained the mechanical and acoustic emission characteristics of coal–rock composites through indoor experiments. Then, we conducted in-depth analysis on the non-uniform deformation behaviors and non-uniform stress field of the coal–rock composite and clarified the generation mechanism of local tensile cracks at the coal–rock interface. Subsequently, we established the energy transfer model of the rock–rock–gas composite specimen in the process of dynamic destabilization in the engineering scale mining field and revealed the mechanism of nonlinear energy evolution and release of the coal–rock–gas composite, which has been less reported in previous studies. In this paper, we further clarified the occurrence and development mechanism of coal–rock–gas compound dynamic disasters in the engineering scale mining environment to guide the prevention and control of coal–rock–gas dynamic disasters in deep mines.

Keywords: deep mines; gas; composite dynamic disaster; energy transfer; mining environment

Citation: Sun, H.; Dai, L.; Lu, J.; Cao, J.; Li, M. Analyzing Energy Transfer Mechanism during Coal and Gas Protrusion in Deep Mines. *Processes* **2022**, *10*, 2634. https://doi.org/10.3390/pr10122634

Academic Editors: Feng Du, Aitao Zhou and Bo Li

Received: 5 November 2022
Accepted: 5 December 2022
Published: 8 December 2022

1. Introduction

For a long time, coal—as the mainstay of energy consumption in China—has played an important role in its social and economic development and will consequently remain irreplaceable for a considerable period of time in the future. However, with the gradual depletion of shallow resources, the mining depth of coal has gradually increased into the Earth's crust and the consequent mining environment presents the characteristics of high crust stress, high gas pressure, and high temperature [1,2]. Deeper mining is accompanied by the obvious appearance of tectonic stress and mining stress [3]. The mechanical and seepage characteristics of coal rocks also show more complex characteristics than those of shallow parts. In addition, with the deterioration of the mining environment, most of the mines show the characteristics of high stress, high gas, and low permeability and deep shaft disasters such as large deformation of the roadways, topping, coal and gas protrusion, coal burst, and compound dynamic disasters that occur frequently. This seriously restricts the safe and efficient mining of deep coal seams [4]. Therefore, a correct understanding of the mechanical properties of deep coal rocks and the understanding of coal–rock disaster

mechanisms are essential for the stability design of the surrounding rock and for the prevention and management of disasters.

Owing to geological structures and stratigraphic movements, rock formations do not exist as a single lithology; laminated rock formations are the most common geological form. The destruction of such composite formations can have a considerable impact on underground engineering activities (mining, excavation, tunneling, geothermal energy extraction, deep burial of nuclear waste, among others) [5]. As a result, many scholars have studied the mechanical behavior of composite coal–rock mass. Particularly in deep thin coal seam mining, studying the mechanical properties of composite coal–rock strata is crucial and the fracture and rupture of the hard roof is very easy to induce the coal–rock dynamic disaster. The composite coal–rock mass is a strong anisotropic material that contains many weak structural surfaces that differ from the properties of the rock matrix. Therefore, studying the mechanical properties and energy release transfer laws of layered composite coal–rock is crucial for revealing the dynamic disaster mechanism of coal and rock in deep mining engineering.

In recent decades, the mechanical properties of layered composite coal rocks have been theoretically and experimentally studied under various stress conditions and there has been considerable progress in this domain. Previous studies have shown that the elastic modulus, Poisson's ratio, deformation behaviors, strength, failure mode, and permeability evolution of layered composite coal–rock are quite different from those of pure rocks, regardless of the stress conditions [5–8]. Dou et al. demonstrated that the elastic modulus and strength of layered composite coal rocks increase with the increase in the height ratio of the rock mass to the coal sample [9]. Tan et al. showed that the rock layer type greatly affects the impact propensity of rock burst. Specifically, the impact tendency of composite coal–rock is proportional to the elastic modulus and strength of the rock [10]. In addition, an applicable method to prevent the collapse of high-velocity impact roofs based on the flexible/hard structure analysis of the composite coal–rock model was proposed [11,12]. The composite rock mass structure is also formed by the backfill after mining. The interaction mechanism between the backfill and the surrounding rock is extremely complex and the failure form shows the characteristics of tensile shear mixing [6]. With the increase in surrounding pressure, the damage mechanism of coal seams in laminated composite coal rocks changes from mixed crack damage to parallel crack damage and finally to single shear crack damage or overall mixed section damage [13,14].

The pre-peak and post-peak deformation and strength behaviors of composite rock mass are closely related to the mechanical properties of the weak rock layer and often play a decisive role; however, the dominant role of this weak structure will gradually decrease with the increase of confining pressure to a certain extent [5,15]. Of course, the control effect of this weak structure and confining pressure is also related to the stress orientation. Through the generalized Poisson's ratio of materials at different locations, the interface confinement effect of composite coal–rock mass was verified. In addition, based on the worst mode, acoustic emission characteristics, the progressive failure mechanism of soft rock–coal combined samples was revealed [15–17]. In addition, the relative change of the contact surface of the coal–rock and the loading orientation of the principal stress will also affect its mechanical behavior. For example, the strength of composite coal–rock tends to be higher in stress perpendicular to the contact surface than parallel to the interface; the rupture is often in the weak coal seam when the stress is parallel to the interface and the opposite may be the overall failure through different rock layers [5,6,18–21]. Furthermore, several studies have investigated the damage, deformation, strength, damage mode, energy evolution, charge induction, acoustic emission, and other characteristics of composite coal–rock bodies under the action of uniaxial, triaxial, cyclic loading, and impact loading stresses [22–27]. While considerable progress has been made in the study of the conventional mechanical behavior of composite coal, there have been few studies on the difference of energy release and transfer between hard rock and coal body during the failure of composite coal, making it necessary to carry out relevant studies. The failure process of rock and coal seams in

coal–rock combination is often not synchronized. After the failure of soft coal seams, the release and transfer of elastic energy of hard rock strata aggravate the secondary failure of weak layers, which are prone to a larger disaster. Consequently, it is necessary to carry out relevant research.

In this work, some uniaxial mechanical tests of coal–rock mass were carried out and the whole process AE characteristics of sample failure were monitored. Then, the effective stress and energy release model of composite coal–rock mass was established. On this basis, the internal process and the mechanism of the occurrence of coal–rock compound dynamic disasters were analyzed.

2. Experimental Study of Energy Transfer during Coal–Rock Composite Dynamic Disaster

Currently, the mechanism of energy transfer and the release of coal–rock multilayer composite structure under the influence of deep mining is unknown, limiting the scope of disaster prevention technology. In response to the overall demand of China's coal mining to move deeper and the need for disaster prevention and control of coal mining under complex high-stress environments, focusing on the coupling action mechanism of high elastic energy of deep-mine quarry perimeter rock systems on coal–rock rupture induction mechanism and coal–rock body energy release at the mining working face, exploring the coupling law of gathering, releasing, and transferring high elastic energy of deep-mine perimeter rock–coal body in the process of composite dynamic disaster initiation, and studying to obtain the quantitative discriminant conditions of coal–rock complex dynamic disaster initiation under high ground stress and mining-induced stress in deep mines are necessary. To this end, we conducted a series of mechanical experimental studies on the coal–rock composite and obtained the characteristics of the total stress–strain relation, acoustic emission energy, and elastic energy dissipation law of the coal–rock composite specimens.

As presented in Figure 1, it is assumed that the failure of each stratification and equivalent whole coal–rock mass conforms to the Mol Coulomb criterion. For pure rocks, it is generally believed that the elastic energy stored before peak is greater than the elastic energy released after peak, and it is considered that dynamic disaster occurs. However, for the composite coal–rock mass, the hard sandstone layer has no overall failure and the accumulated elastic energy can bounce back and transfer energy to the coal seam after the failure of the soft coal seam. It can be assumed that the rebound energy of the hard sandstone is greater than the energy required for the fracture of the damaged coal seam per unit post-peak and a disaster will occur.

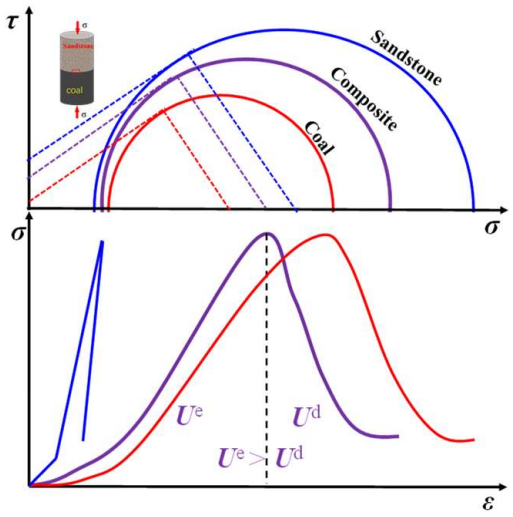

Figure 1. Failure and disaster discrimination model of composite coal–rock mass (U^e is the pre-peak stored elastic energy; U^d is the post-peak dissipation elastic energy).

2.1. Mechanical Characteristics of the Coal–Rock Assemblage

Uniaxial mechanical tests were conducted using raw coal and roof sandstone from a typical mine in Shanxi, and coal–rock assemblage tests with different lithologies and thicknesses were conducted to gain insight into the differences in the layered mechanical behaviors and strength response characteristics of the assembled coal–rock bodies. The height of the coal seam collapse zone of the sandstone roof is 1–2 times that of the coal seam, thus the height ratio of 1:1, 3:2, and 2:1 for coal to sandstone were investigated. The test principle is shown in Figure 2. The experiments are based on PIC2 acoustic emissions (PAC, Princeton Jct, NJ, USA) to monitor their micro–seismic properties.

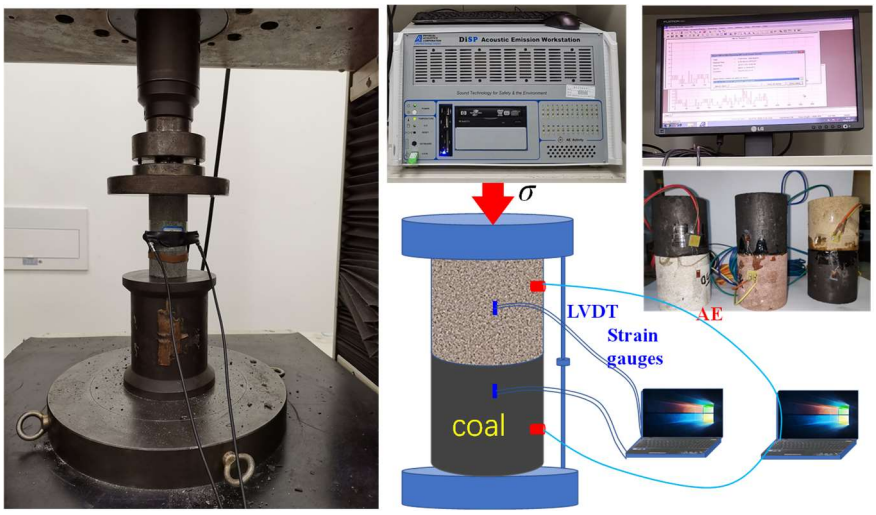

Figure 2. Principle of uniaxial mechanical testing of combined coal bodies.

The strength evolution characteristics of the combined coal bodies of different sandstone types are given in Figure 3. The figure shows that the compressive strength of the fine sandstone assemblage is greater than that of the coarse sandstone assemblage, and the strength of both is lower than that of the siltstone assemblage. In other words, the strength of the siltstone and coal assemblage is greater for the same proportion of the assemblage, which is mainly influenced by the strength of the other components except coal, and the greater the strength of the sandstone, the greater the overall strength of the assemblage. On the contrary, the strength of the composite is close to that of coal. Although it is increased, the range is small. Therefore, it can be judged that the strength of the composite mainly depends on the strength of the weak coal.

This is mainly because the deformation modulus and Poisson's ratio of sandstone and coal are different, resulting in the constraint stress at the interface of the coal–rock mass [5,24]. As shown in Figure 1, the effective cohesion stress and internal friction angle of the combined coal–rock mass are greater than those of a pure coal layer, so its overall equivalent strength would be improved, as presented Figure 3.

The strength law of the assemblage under different coal–rock thickness ratio conditions is given in Figure 4. The figure shows that the compressive strength gradually increases with the climbing rock–coal height ratio. This also indicates that the strength of the assemblage increases to different degrees as the rock–coal height ratio increases. When the rock–coal ratio increased from 1:1 to 3:2 and 2:1, the strength of the coal–rock assemblage increased from 5.745 MPa to 5.985 and 6.225 MPa in that order, which is an increase of 4.176% and 8.355%, respectively. For the coal–rock assemblage, its strength is not only affected by lithology but also the coal–rock thickness ratio exudes some influence.

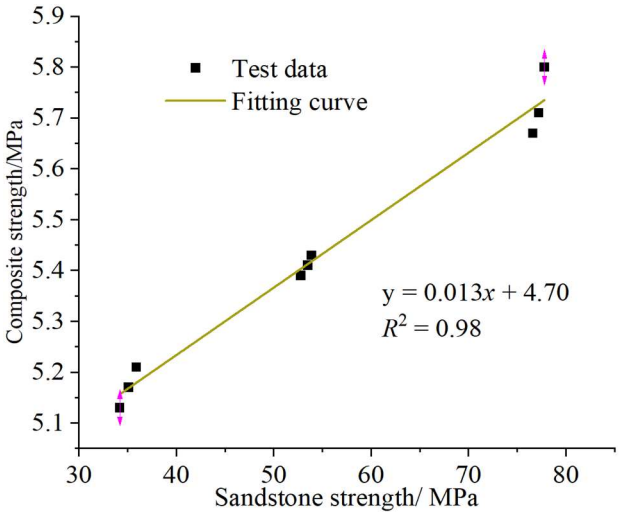

Figure 3. Effect of lithology on the strength of coal–rock assemblages.

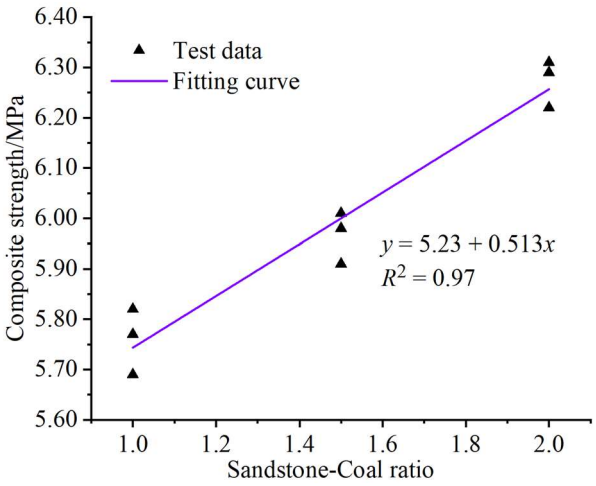

Figure 4. Effect of coal–rock thickness ratio on the strength of the coal–rock assemblage.

The relation between the maximum instantaneous release of acoustic emission energy and the lithology and thickness ratio of the coal–rock assemblage is given in Figure 5, showing that with the increase of the sandstone layer strength, the AE transient energy maximum shows an increasing trend and, with the increase in the rock–coal thickness ratio, the AE energy maximum transient release also shows an increasing trend, which is consistent with the change in the coal–rock assemblage strength. This indicates that the greater the strength of the coal–rock assemblage, the more energy is stored before the peak and the greater the peak instantaneous release energy is, i.e., the greater the chance of a coal–rock dynamic hazard. In actual engineering, due to the influence of mining disturbance, the rock body ruptures and releases energy and the amount of instantaneous released energy directly determines the intensity of the dynamic hazard. In deep coal mining, the probability and energy level of impact disaster will be considerably increased for hard roof and thick roof deposit conditions, which should be prevented and regulated in a timely manner.

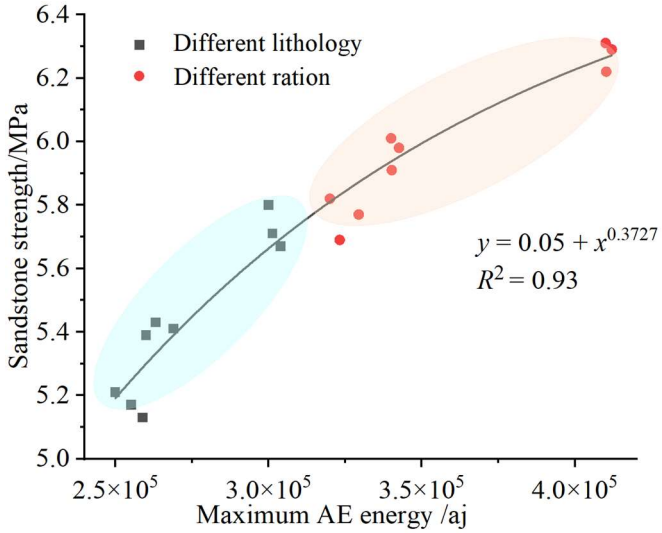

Figure 5. Maximum transient energy versus coal–rock assemblage structure.

2.2. Non–Uniform Deformation Behavior of Coal–Rock Assemblage

In this work, strain gauges were installed in sandstone and coal layers, respectively, to monitor the deformation of each layer and the deformation of the whole assembly was monitored by the axial displacement meter of the instrument. Due to the differences in the mechanical properties of the sandstone and the raw coal stratification in the coal–rock assemblage, there are large differences in the deformation of each stratification under uniaxial stress conditions. Figure 6 gives the deformation relation of sandstone and raw coal layering and the combination of different lithological coal–rock combinations (one of the specimens is selected for analysis for each experimental condition). For different lithological combinations, the deformation of the composite coal–rock body is always between the deformation of sandstone and raw coal fractal, and the deformation of raw coal fractal is much larger than that of sandstone fractal. As the strength of the sandstone layer increases, the deformation of the sandstone fractal is lower and the deformation of the coal fractal is greater simultaneously. In addition, after the peak, the deformation of the original coal fractal and the assemblage continues to increase, while the deformation of the sandstone fractal gradually decreases.

The analysis concluded that for the coal–rock assemblage, the raw coal delamination strain is much larger than the sandstone delamination under the same uniaxial stress because the modulus of elasticity and strength of the raw coal are much lower than that of the sandstone. When the raw coal partition enters the yielding and post-peak stage, the sandstone partition is still in the elastic stage, the post-peak stress decreases, and the strain decreases for the sandstone partition due to elastic rebound, whereas the strain continues to increase for the raw coal due to post-peak fracture surface slip. In addition, for sandstone layering elastic rebound, this effect exacerbates the damage and destruction of the raw coal layering. That is, after the overall destabilization of the coal–rock assemblage specimen occurred, the rupture occurred mainly in the coal stratum, while the elastic deformation energy originally stored in the sandstone stratum occurred due to the overall stress reduction and deformation rebound phenomenon; this deformation acted on the coal stratum and accordingly prompted the development of fractures in the coal.

In the actual deep coal seam mining process, the coal mass in front of the working face was damaged and broken due to mining disturbance, and the elastic energy transfer from the hard roof is easy to trigger the coal seam to produce a large number of fractures, thus increasing permeability of the coal seam, thus increasing the gas outburst risk. In addition, roof elastic energy transfer would also aggravate the fracture of the coal seam, resulting in an instability coal-burst disaster.

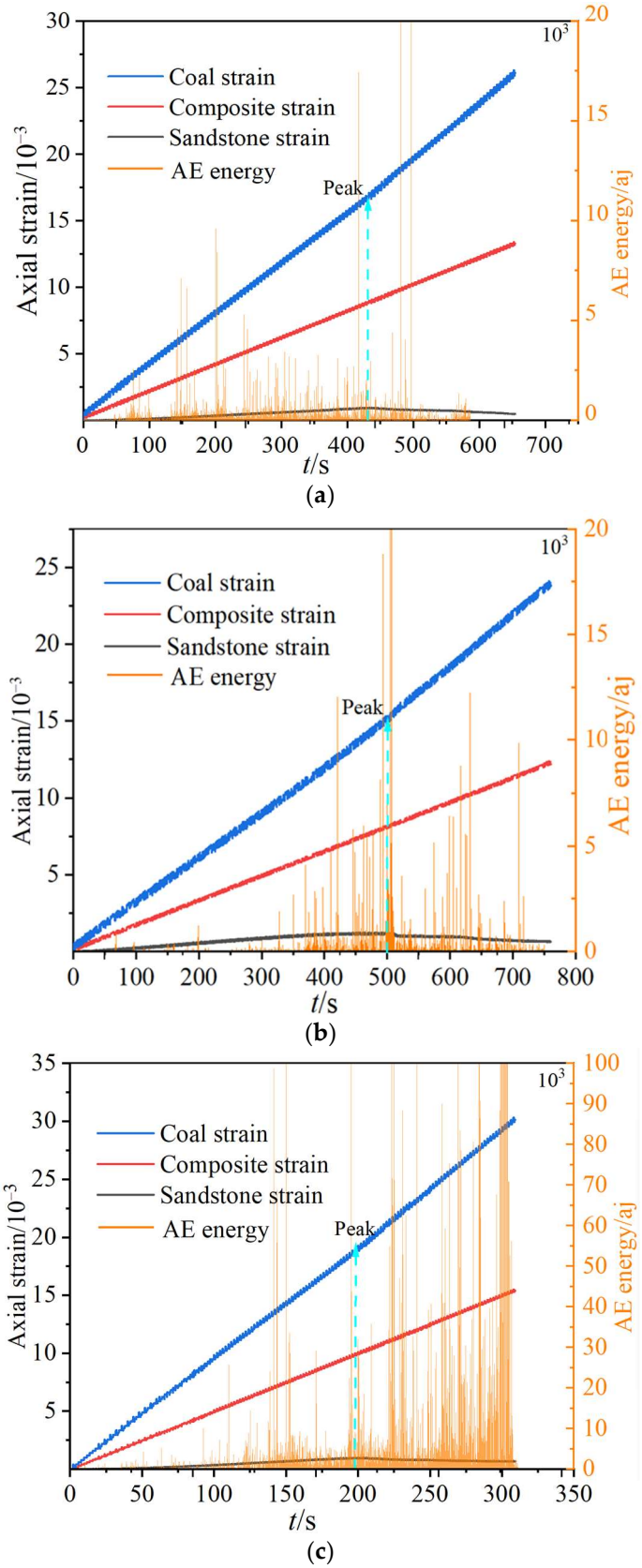

Figure 6. Strain relation between sandstone and coal stratification of specimens with different lithological coal rock combinations. (**a**) coarse sandstone–coal; (**b**) siltstone–coal; (**c**) fine sandstone–coal.

3. Analysis of the Local Non-Uniform Stress Field in the Coal–Rock Assemblage

In fact, during the deformation and damage of the assemblage, the coal body can be considered to be subjected to the 'surrounding pressure' of the rock near the joint surface, whereas the rock body near the joint surface is subjected to radial tension. Of course, the surrounding pressure mentioned here is not the radially uniform surrounding pressure applied to the side of the specimen during the triaxial test. The pressure exerted by the triaxial test can be regarded as the active pressure, while the coal body part is subjected to the 'pressure-supporting effect' only when the coal body part is radially deformed by the axial load on the combined specimen, which is, in a sense, the 'passive pressure-supporting effect'. It is spatially distributed in the coal part near the joint surface and varies with the degree of deformation.

The stresses and deformations of each laminated rock in the composite coal rock are very different from those of the intact individual rocks. To maintain the same deformation of the composite coal–rock samples under triaxial compressive stress, the lateral deformation of the weaker rock is constrained by the stronger rock. Due to the difference in sandstone–coal deformation and the coordinated constraint of interfacial deformation, the sandstone will limit the deformation of coal specimens with smaller lateral deformations and reduce its deformation. Conversely, coal specimens with large lateral deformations will promote the deformation of sandstone with smaller lateral deformations and increase its deformation. This also results in the strength of the composite coal–rock body being higher than that of the coal specimen and lower than that of the sandstone specimen. Based on the stress balance relation, the three principal stresses in each layer should satisfy the following relation [24]:

$$\begin{cases} \sigma_1^R = \sigma_1, \sigma_1^C = \sigma_1 \\ \sigma_2^R = \sigma_2 + \sigma_{2p}^R, \sigma_2^C = \sigma_2 + \sigma_{2p}^C \\ \sigma_3^R = \sigma_3 + \sigma_{3p}^R, \sigma_3^C = \sigma_3 + \sigma_{3p}^C \end{cases} \tag{1}$$

where $\sigma_1^R, \sigma_2^R, \sigma_3^R, \sigma_1^C, \sigma_2^C, \sigma_3^C$ are the three effective principal stresses of rock and coal seam are represented, respectively.$\sigma_{2p}^R, \sigma_{3p}^R, \sigma_{2p}^C, \sigma_{3p}^C$ denote the confining stresses in the directions of σ_2 and σ_3 for the sandstone and coal samples, respectively.

The additional stresses caused by the principal stresses satisfy the following relation [24]:

$$\begin{cases} \sigma_{2p}^R = -\sigma_{2p1}^R + \sigma_{2p2}^R - \sigma_{2p3}^R \\ \sigma_{3p}^R = -\sigma_{3p1}^R - \sigma_{3p2}^R + \sigma_{3p3}^R \\ \sigma_{2p}^C = \sigma_{2p1}^C - \sigma_{2p2}^C + \sigma_{2p3}^C \\ \sigma_{3p}^C = \sigma_{3p1}^C + \sigma_{3p2}^C - \sigma_{3p3}^C \end{cases} \tag{2}$$

where $\sigma_{2p1}^R, \sigma_{2p2}^R, \sigma_{2p3}^R, \sigma_{2p1}^C, \sigma_{2p2}^C, \sigma_{2p3}^C$ are the induced confining stresses caused by three principal stresses in sandstone and coal samples.

At the laminated contact surfaces of coal and rock, the additional stresses between coal and rock are the same due to cementation. Therefore, the additional stresses should satisfy the following relation [24].

$$\begin{cases} \sigma_{2p1}^R = \sigma_{2p1}^C, \sigma_{2p2}^R = \sigma_{2p2}^C, \sigma_{2p3}^R = \sigma_{2p3}^C \\ \sigma_{3p1}^R = \sigma_{3p1}^C, \sigma_{3p2}^R = \sigma_{3p2}^C, \sigma_{3p3}^R = \sigma_{3p3}^C \end{cases} \tag{3}$$

As described in Figure 7, for uniaxial compressive stress states ($\sigma_2 = \sigma_3 = 0$):

$$\begin{cases} \sigma_c^2 = \sigma_c^3 = -\sigma_t^2 = -\sigma_t^3 \\ \sigma_1^R = \sigma_1^C = \sigma \end{cases} \tag{4}$$

According to the generalized Hooke's law,

$$\begin{cases} \varepsilon_2^R = \frac{1}{E_R}\left[\sigma_c^2 - v_R(\sigma_1^R + \sigma_c^3)\right] \\ \varepsilon_3^R = \frac{1}{E_R}\left[\sigma_c^3 - v_R(\sigma_1^R + \sigma_c^2)\right] \\ \varepsilon_2^C = \frac{1}{E_C}\left[-\sigma_t^2 - v_C(\sigma_1^C - \sigma_t^3)\right] \\ \varepsilon_3^C = \frac{1}{E_C}\left[-\sigma_t^3 - v_C(\sigma_1^C - \sigma_t^2)\right] \end{cases} \tag{5}$$

where $\varepsilon_2^R, \varepsilon_3^R, \varepsilon_2^C, \varepsilon_3^C$ represents the strain of the rock and coal seam in the direction of stress σ_2, σ_3, respectively. E_R, E_C, v_R, v_C are the elastic modulus and Poisson's ratio of the rock and coal layer, respectively.

Assuming that both the rock and coal seams are transverse isotropic, the strain satisfied:

$$\begin{cases} \varepsilon_2^R = \varepsilon_2^C \\ \varepsilon_3^R = \varepsilon_3^C \end{cases} \tag{6}$$

Subsequently,

$$\begin{cases} \sigma_1^R = \sigma_1^C = \sigma \\ \sigma_c^2 = \sigma_c^3 = -\sigma_t^2 = -\sigma_t^3 = \frac{E_C v_R - E_R v_C}{E_R(1-v_C) + E_C(1-v_R)}\sigma \end{cases} \tag{7}$$

Based on the above analysis, the stress characteristics of each part of the coal–rock assemblage can be clearly understood and the generation mechanism of local tensile cracks at the coal–rock interface can be better understood.

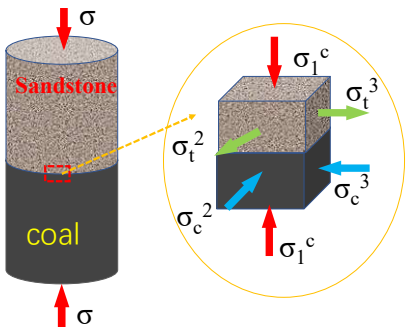

Figure 7. Local stress analysis of the coal–rock assemblage.

4. Energy Nonlinear Evolution and Release Mechanisms of Coal–Rock Assemblages

To study the destabilization and damage mechanism of the coal–rock assemblage under dynamic action and to explore the interaction relation between coal–rock components, a deformation and energy evolution model of coal–rock assemblage was constructed, as shown in Figure 8.

The coal and rock components constitute the coal–rock assemblage, which is kept in mechanical equilibrium under the load σ. The load-displacement curves of the rock component and the coal component can be expressed by Equation (7). The strength of the rock component is stronger than that of the coal component so that destabilization damage did not occur and the stress–strain relation of the coal (c) and the sandstone (s) layer is as follows [11].

$$\begin{cases} \sigma_c = E_C \varepsilon_c \\ \sigma_s = E_S \varepsilon_s \end{cases} \tag{8}$$

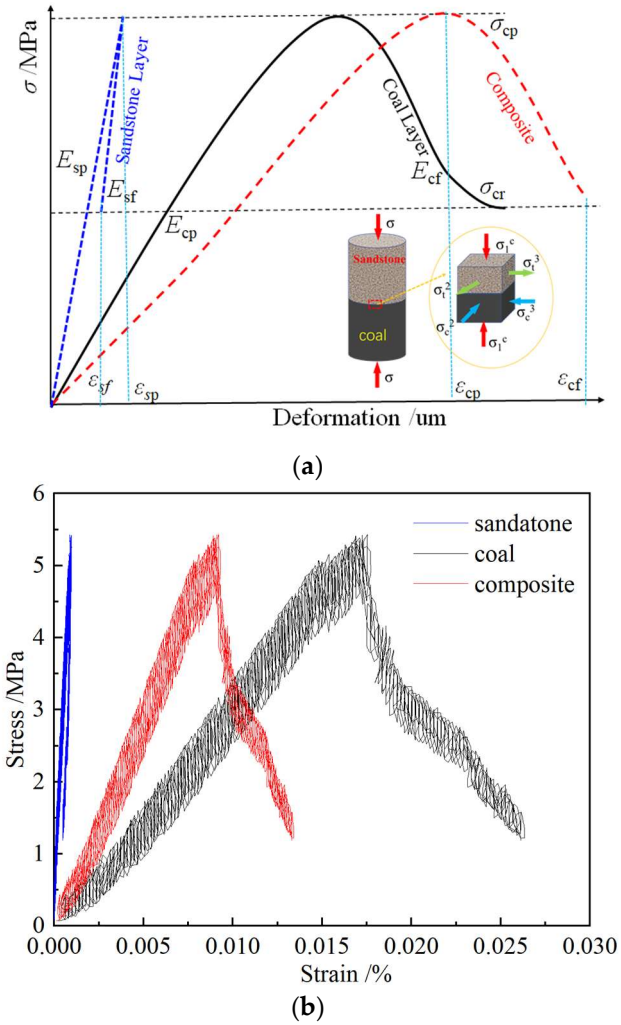

Figure 8. Deformation model of coal–rock assemblage. (**a**) Composite coal–rock deformation diagram; (**b**) strain test results of composite coal–rock mass.

Assuming that the components and assemblies satisfy the law of energy conservation during stress loading and that the temperature field remains constant, the peak front energy field relation should satisfy the following relation [28,29].

$$\begin{cases} U_T = U_c + U_s = \int_0^{\varepsilon_{cp}} \sigma_c d\varepsilon_c + \int_0^{\varepsilon_{sp}} \sigma_s d\varepsilon_s \\ U_T^e = U_c^e + U_s^e = \frac{\sigma^2}{2E_C} + \frac{\sigma^2}{2E_S} \\ U_T^d = U_c^d + U_s^d = U_T - U_T^e \end{cases} \tag{9}$$

where U_T, U_c, U_s are the total energy of composite, coal, and sandstone layer, respectively; U_T^e, U_c^e, U_s^e are the elastic energy of composite, coal, and sandstone layer, respectively; U_T^d, U_c^d, U_s^d are the dissipate energy of composite, coal, and sandstone layer, respectively.

Combined with Figure 8, it can be seen that the energy relation between the peak to post-peak residual phase of raw coal stratification is satisfied.

$$\begin{cases} \Delta U_c^e = U_{cp}^e - U_{cf}^e = \frac{{\sigma_{cp}}^2}{2E_{cp}} - \frac{{\sigma_{cf}}^2}{2E_{cf}} \\ \Delta U^d = U_{cp} - U_{cf} \end{cases} \tag{10}$$

where U_{cp}^{e}, U_{cf}^{e} are the elastic energy before and after peak stress; σ_{cp}, σ_{cf} are the peak and residual strength of composite coal–rock; E_{cp}, E_{cf} are the elastic modulus before and after peak stress; ΔU^{d} and U_{cf} are the elastic energy and total mechanical energy that can be released at the residual strength of the raw coal stratification, respectively.

For the peak to post-peak residual phase of sandstone layer, the energy relation can be obtained:

$$\Delta U_{s}^{e} = U_{sp}^{e} - U_{sf}^{e} = \frac{\sigma^2}{2E_{sp}} - \frac{\sigma^2}{2E_{sf}} \tag{11}$$

It is assumed that all deformation energy of the elastic rebound of the sandstone partition is transferred to the original coal partition. Based on this, the energy transferred from (DU^{dd}) the sandstone partition to the original coal partition in the post-peak phase is:

$$DU^{dd} = U_{cp}^{e} - U_{cf}^{e} = \frac{{\sigma_{cp}}^2}{2E_{sp}} - \frac{{\sigma_{cf}}^2}{2E_{sf}} \tag{12}$$

where E_{sp}, E_{sf} denote the loaded and unloaded modulus of elasticity of sandstone stratification, respectively; σ_{cp}, σ_{cf} denote the peak and residual strength of coal–rock assemblage, respectively.

Figure 9 shows a model of non-linear energy transfer and release rupture of the coal–rock assemblage. The main reason for this is that the assemblage is continuously loaded by the testing machine and, although there is a loss of energy, a considerable amount of energy is accumulated overall. As the energy storage limit of the coal component is low, the weak coal component is the first to break when the accumulated energy reaches the energy storage limit of the assemblage. In this manner, a considerable amount of elastic energy is released and the overall stress is reduced. Owing to the coordinated tensile effect of the rock–coal interface, tiny cracks are formed on the surface of the rock component (which is prone to tensile damage), the stress is reduced after the peak of the assemblage, and the elastic rebound of the sandstone stratum occurs due to stress reduction. Thus, the elastic energy of the sandstone stratum is transferred to the original coal stratum. This leads to the intensified damage of the original coal stratum and is more prone to coal–rock dynamic disaster or secondary dynamic impact disaster.

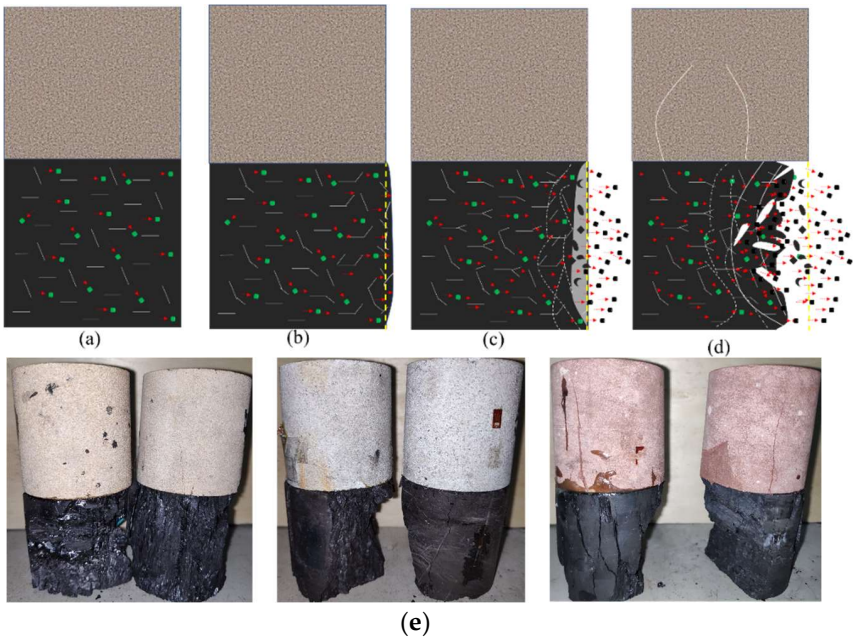

Figure 9. Non-linear energy transfer and release rupture-causing model for coal–rock assemblages. ((**a**–**d**), Incongruous fracture evolution of composite coal rock mass; (**e**) failure modes of composite coal-rock of the experiments).

Therefore, in the actual process of deep resources development, it is necessary to avoid the sudden rupture of hard roof caused by mining disturbance and reasonable and effective measures should be taken to support the roof or to relieve stress in a timely manner.

5. Conclusions

In order to solve the complicated problem of coupling failure disaster mechanisms of the special structure of hard–roof soft–coal seams in the deep coal mining process, this work carried out experimental and theoretical research and revealed the coupling fracture behavior and the energy transfer law of the coal–rock assemblage. The main conclusions are as follows:

(1) The mechanical behaviors of the combined coal–rock body are different from that of a single coal–rock. Particularly, the overall strength of the combined coal–rock body is higher than that of a single raw coal, which is of great significance to the actual deep coal mine in terms of roof control and surrounding rock support.
(2) The damage of the coal–rock assemblage in the uniaxial stress state occurs mainly in the soft raw coal stratification, and the sandstone part of the hard roof is in the elastic stage throughout the process. The elastic rebound after the overall destabilization transfers energy to the coal seam.
(3) The effective stress relation of each stratum of the combined coal–rock body was obtained based on the deformation coordination relation, and the coal–rock body rupture roof coal seam elastic energy transfer relation was obtained based on this. The hard roof often transferred part of its stored elastic energy to the coal seam after the coal seam was unstable, thus aggravating the coal seam instability.

The research of this work is of great significance for the safe mining of deep hard roof coal seams, disaster prevention and control, and may provide important theoretical reference. The work in this paper is mainly based on the uniaxial compression condition to establish a mathematical model, therefore it is necessary to consider the influence of three-dimensional stress fields in the future, as the failure mechanism and energy transfer law are more complex.

Author Contributions: Conceptualization, H.S.; methodology, H.S., L.D., J.L. and M.L.; validation, H.S., L.D., J.L. and M.L.; formal analysis, J.C.; investigation, L.D. and J.L.; resources, H.S.; data curation, L.D. and J.L.; writing—original draft preparation, H.S., L.D., J.L. and M.L.; writing—review and editing, H.S., L.D., J.L., J.C. and M.L.; visualization, L.D. and J.L.; supervision, H.S. and M.L.; project administration, L.D. and J.C.; funding acquisition, H.S. and L.D. All authors have read and agreed to the published version of the manuscript.

Funding: This research was funded by National Natural Science Foundation of China (No. 51874348, No. 52104239), Chongqing Science Fund for Distinguished Young Scholars (No. cstc2019jcyjjqX0019), Natural Science Foundation of Chongqing (No. CSTB2022NSCQ-MSX1080).

Institutional Review Board Statement: Not applicable.

Informed Consent Statement: Not applicable.

Data Availability Statement: All data and/or models used in the study appear in the submitted article.

Conflicts of Interest: The authors declare no conflict of interest.

References

1. Li, W.; Liu, J.; Zeng, J.; Leong, Y.K.; Elsworth, D.; Tian, J. A fully coupled multidomain and multiphysics model considering stimulation patterns and thermal effects for evaluation of coalbed methane (CBM) extraction. *J. Pet. Sci. Eng.* **2022**, *214*, 110506. [CrossRef]
2. Wang, L.; Cheng, Y.P.; Ge, C.G.; Chen, J.X.; Li, W.; Zhou, H.X.; Wang, H.F. Safety technologies for the excavation of coal and gas outburst-prone coal seams in deep shafts. *Int. J. Rock Mech. Min. Sci.* **2013**, *57*, 24–33. [CrossRef]
3. Du, F.; Wang, K.; Guo, Y.Y.; Wang, G.D.; Wang, L.; Wang, Y.H. The mechanism of rockburst-outburst coupling disaster considering the coal-rock combination: An experiment study. *Geomech. Eng.* **2020**, *22*, 255–264.

4. Dai, L.; Zhang, Z.; Sun, H.; Gao, H. Research on mechanical properties and energy evolution law of coal–rock assemblage with different gas pressures. *Sustainability* **2022**, *14*, 9904. [CrossRef]
5. Lu, J.; Huang, G.; Gao, H.; Li, X.; Zhang, D.M.; Yin, G.Z. Mechanical properties of layered composite coal–rock subjected to true triaxial stress. *Rock Mech. Rock Eng.* **2020**, *53*, 4117–4138. [CrossRef]
6. Cui, B.Q.; Feng, G.R.; Bai, J.W.; Wang, K.; Shi, X.D.; Wu, H.T. Acoustic emission characteristics and damage evolution process of backfilling body–coal pillar–backfilling body composite structure. *Bull. Eng. Geol. Environ.* **2022**, *81*, 300. [CrossRef]
7. Du, F.; Wang, K.; Wang, G.D.; Jiang, Y.F.; Xin, C.P.; Zhang, X. Investigation of the acoustic emission characteristics during deformation and failure of gas-bearing coal-rock combined bodies. *J. Loss Prev. Process Ind.* **2018**, *55*, 253–266. [CrossRef]
8. Liu, Y.; Lu, C.P.; Liu, B.; Xiao, Z.Y.; Zhang, H. Slip and instability mechanisms of coal-rock parting-coal structure (CRCS) under coupled dynamic and static loading. *Energy Sci. Eng.* **2019**, *7*, 2703–2719. [CrossRef]
9. Dou, L.M.; Lu, C.P.; Mu, Z.L.; Zhang, X.T.; Li, Z.H. Rock burst tendency of coal-rock combinations sample. *J. Mine Saf. Eng.* **2006**, *23*, 43–46.
10. Tan, Y.L.; Liu, X.S.; Shen, B.; Ning, J.G.; Gu, Q.H. New approaches to testing and evaluating the impact capability of coal seam with hard roof and/or floor in coal mines. *Geomech. Eng.* **2018**, *14*, 367–376.
11. Liu, X.S.; Tan, Y.L.; Ning, J.G.; Lu, Y.W.; Gu, Q.H. Mechanical properties and damage constitutive model of coal in coal-rock combined body. *Int. J. Rock Mech. Min. Sci.* **2018**, *110*, 140–150. [CrossRef]
12. Tan, Y.L.; Yu, F.H.; Ning, J.G.; Zhao, T.B. Design and construction of entry retaining wall along a gob side under hard roof stratum. *Int. J. Rock Mech. Min. Sci.* **2015**, *77*, 115–121. [CrossRef]
13. Zuo, J.P.; Wang, Z.F.; Zhou, H.W.; Pei, J.L.; Liu, J.F. Failure behavior of a rock-coal-rock combined body with a weak coal interlayer. *Int. J. Min. Sci. Technol.* **2013**, *23*, 907–912. [CrossRef]
14. Zhao, Z.H.; Wang, W.M.; Dai, C.Q.; Yan, J.X. Failure characteristics of three-body model composed of rock and coal with different strength and stiffness. *Trans. Nonferrous Met. Soc. China* **2014**, *24*, 1538–1546. [CrossRef]
15. Song, H.Q.; Zuo, J.P.; Liu, H.Y.; Zuo, S.H. The strength characteristics and progressive failure mechanism of soft rock-coal combination samples with consideration given to interface effects. *Int. J. Rock Mech. Min. Sci.* **2021**, *139*, 104593. [CrossRef]
16. Jiang, Y.L.; Lian, H.J.; Nguyen, V.P.; Liang, W.G. Propagation behavior of hydraulic fracture across the coal-rock interface under different interfacial friction coefficients and a new prediction model. *J. Nat. Gas Sci. Eng.* **2019**, *68*, 102894. [CrossRef]
17. Li, C.J.; Xu, Y.; Zhang, Y.T.; Li, H.L. Study on the energy evolution and fractal characteristics of fracture-like coal rock assemblages under impact loading. *J. Rock Mech. Eng.* **2019**, *38*, 2231–2241.
18. Liu, Y.; Lu, C.P.; Zhang, H.; Wang, H.Y. Numerical investigation of slip and fracture instability mechanism of coal- rock parting-coal structure (CRCS). *J. Struct. Geol.* **2019**, *118*, 265–278. [CrossRef]
19. Bai, J.W.; Feng, G.R.; Wang, Z.H.; Wang, S.Y.; Qi, T.Y.; Wang, P.F. Experimental investigations on the progressive failure characteristics of a sandwiched coal-rock system under uniaxial compression. *Appl. Sci.* **2019**, *9*, 1195. [CrossRef]
20. Wang, K.; Du, F.; Zhang, X.; Wang, L.; Xin, C.P. Mechanical properties and permeability evolution in gas-bearing coal-rock combination body under triaxial conditions. *Environ. Earth Sci.* **2017**, *76*, 815. [CrossRef]
21. Cheng, H.M.; Zhang, N.; Yang, Y.G.; Dong, Y.X.; Peng, W.H. 3D dynamic evolution analysis of coal-rock damaged field and gas seepage field during the gas extraction process. *J. Nat. Gas Sci. Eng.* **2018**, *56*, 444–454. [CrossRef]
22. Li, L.P.; Wu, J.P.; Ju, X.Y.; Wang, L. Analysis of ultra-low friction effect of combined coal rock under the action of surrounding pressure and impact disturbance. *J. Geomech.* **2019**, *25*, 1099–1106.
23. Li, N.; Huang, B.X.; Zhang, X.; Tan, Y.Y.; Li, B.L. Characteristics of microseismic waveforms induced by hydraulic fracturing in coal seam for coal rock dynamic disasters prevention. *Saf. Sci.* **2019**, *115*, 188–198. [CrossRef]
24. Lu, J.; Yin, G.Z.; Deng, B.Z.; Zhang, W.Z.; Li, M.H.; Chai, X.W.; Liu, C.; Liu, Y.B. Permeability characteristics of layered composite coal-rock under true triaxial stress conditions. *J. Nat. Gas Sci. Eng.* **2019**, *66*, 60–76. [CrossRef]
25. Xiao, X.C.; Fan, Y.F.; Wu, D.; Ding, X.; Wang, L.; Zhao, B.Y. Energy dissipation characteristics of combined coal rock damage process and impact hazard evaluation. *Geotech. Mech.* **2019**, *40*, 4203–4212, 4219.
26. Yin, G.Z.; Li, X.; Lu, J.; Song, Z.L. Damage criterion for layered composite rocks under true triaxial stress conditions. *J. Rock Mech. Eng.* **2017**, *36*, 261–269.
27. Zuo, J.P.; Chen, Y.; Cui, F. Differences in mechanical properties and impact propensity analysis of different coal rock assemblages. *J. China Univ. Min. Technol.* **2018**, *47*, 81–87.
28. Lu, J.; Yin, G.Z.; Gao, H.; Li, X.; Zhang, D.M.; Deng, B.Z.; Wu, M.Y.; Li, M.H. True triaxial experimental study of disturbed compound dynamic disaster in deep underground coal mine. *Rock. Mech. Rock. Eng.* **2020**, *53*, 2347–2364. [CrossRef]
29. Xie, H.P.; Lu, J.; Li, C.B.; Li, M.H.; Gao, M.Z. Experimental study on the mechanical and failure behaviors of deep rock subjected to true triaxial stress: A review. *Int. J. Min. Sci. Technol.* **2022**, *32*, 915–950. [CrossRef]